The effect of heat- and auto-polymerized denture base polymers on clonogenicity, apoptosis, and necrosis in fibroblasts: denture base polymers induce apoptosis and necrosis

Mihaela Roxana Cimpan, Roald Matre, Lill Irene Cressey, Berit Tysnes,
Stein Atle Lie, Bjørn Tore Gjertsen and Nils Skaug

Department of Odontology—Dental Biomaterials, Faculty of Dentistry, University of Bergen, Bergen, Norway; Department of Microbiology and Immunology, The Gade Institute, Faculty of Medicine, University of Bergen, Bergen, Norway; The Faculty of Health Studies, Sogn and Fjordane College, Førde, Norway; Department of Anatomy and Cell Biology, Faculty of Medicine, University of Bergen, Bergen, Norway; Division of Statistics, Faculty of Medicine, University of Bergen, Bergen, Norway; Department of Odontology—Oral Microbiology, Faculty of Dentistry, University of Bergen, Bergen, Norway; Centre for International Health, University of Bergen, Bergen, Norway

Cimpan MR, Matre R, Cressey LI, Tysnes B, Lie SA, Gjertsen BT, Skaug N. The effect of heat- and auto-polymerized denture base polymers on clonogenicity, apoptosis, and necrosis in fibroblasts: denture base polymers induce apoptosis and necrosis. Acta Odontol Scand 2000;58:217–228. Oslo. ISSN 0001-6357.

Eluates from poly(methyl methacrylate)-based denture base polymers have recently been found to enhance death by apoptosis and necrosis in U-937 human monoblastoid cells. The present study investigated the potential of such polymers to induce apoptosis and/or necrosis and to alter clonogenicity in L929 murine fibroblasts. A fibroblast cell line was chosen because the impairment of fibroblasts subjacent to denture bases may result in a weaker or more permeable mucosa. Two aspects were addressed: the effect of direct contact with the denture base polymers and the effect of eluates extracted from the polymers. For this purpose L929 fibroblasts were seeded on disks manufactured from three heat-polymerized and four autopolymerized denture base polymers or in different concentrations of their eluates. The effects were evaluated by light, fluorescent, confocal and electron microscopy, counting of colonies, and flow cytometry. Disks and eluates of all polymers enhanced cell death by apoptosis and necrosis in L929 cells and decreased their clonogenic potential in a dose-dependent manner. Apoptosis was the main form of cell death. In general, the deleterious effects were stronger when cells were plated directly on the polymer disks than in the eluates. The autopolymerized polymers, except one, yielded higher percentages of apoptosis and necrosis than the heat-polymerized polymers. The results of the study indicated that poly(methyl methacrylate)-based denture base polymers trigger death-signals in L929 fibroblasts and open doors for possible modulation of the cell/biomaterial interaction. □ *Apoptosis; clonogenicity; denture base polymers; necrosis*

Mihaela Roxana Cimpan, Department of Odontology—Dental Biomaterials, Faculty of Dentistry, Aarstadveien 17, N-5009 Bergen, Norway. Tel. +47 5597 4601, fax. +47 5597 4689, e-mail. Mihaela-Roxana.Cimpan@cih.uib.no

Poly(methyl methacrylate) (PMMA)-based denture base polymers, some of the most widely used synthetic polymers for manufacturing denture bases (1), have shown various degrees of cytotoxicity in vitro (2–5). Recently, eluates from PMMA-based denture base polymers have been shown to activate death-signaling pathways in the U-937 human monoblastoid cells (6). However, the reactions of cells in contact with the material surface with regard to the mechanisms of cell death remain to be elucidated. This is an important aspect, since the future of biomaterials' science, as outlined by Ratner (7), lies in the capacity to produce the desired interfacial (i.e. tissue/biomaterial) reaction. It is important to test the death-inducing potential of a biomaterial in different cell lines, since it is known that different cell types may exhibit a wide spectrum of responses to the same toxic stimulus with regard to susceptibility, kinetics of the toxic effect, or mode of cell death.

Two main forms of cell death have been described: apoptosis and necrosis (8). Apoptosis is an active and physiological process characterized by cell shrinkage, detachment from neighboring cells, condensation of nuclear chromatin followed by nuclear fragmentation, and preservation of the structural integrity and most of the functions of the plasma membrane and of the cellular organelles. In vivo, apoptotic cells are rapidly phagocytized without triggering an inflammatory reaction. In vitro, in the absence of professional phagocytes, the apoptotic cells eventually swell and finally cell lysis occurs. This late stage of in vitro apoptosis was named 'secondary necrosis', and more recently 'apoptotic necrosis' (9). Necrosis is a passive and degenerative process occurring as a result of the cell's exposure to gross injury. It is characterized by mitochondrial swelling, dissolution of the nucleus, rupture of the plasma membrane, and release of the cytoplasmic constituents. Necrosis triggers an inflammatory reaction in the tissue and often results in scar formation (9). Signals that under normal circumstances cause apoptosis will in a situation with low adenosine triphosphate (ATP) result in necrosis (10). Cell death phenotypes, which do not fit

218 *M. R. Cimpan et al.*   ACTA ODONTOL SCAND 58 (2000)

strictly into a definition of apoptosis and necrosis, have been previously reported (11, 12). It is therefore important to use different methods for defining the characteristics of cell death induced by a particular agent in a particular cell type.

A recently developed method for detection of apoptosis relies on the specific binding of Annexin V to phosphatidylserine (PS) (13). During apoptosis PS is translocated to the outer layer of the cell membrane. Apoptosis can also be quantified by staining with the DNA binding dye propidium iodide (PI) based on the fact that fixed, permeabilised apoptotic cells have a reduced DNA content and therefore, a low DNA stainability with PI (14). One of the most generally accepted and sensitive methods of assaying for cell survival is the ability of isolated cells to form colonies (15). To avoid ambiguities regarding the mode of cell death, morphological criteria are usually employed for identification of apoptotic and necrotic cells (14).

The objective of the present study was to explore the hypothesis that PMMA-based denture base polymers affect the clonogenicity and induce death by apoptosis and/or necrosis in L929 fibroblasts. Two aspects were addressed: the effect of direct contact with the denture base polymers and the effect of eluates extracted from the polymers. The effects were evaluated by light, fluorescent, confocal and electron microscopy, counting of colonies, and flow cytometry.

Materials and methods

Denture base polymers

Commercially available heat-polymerized and autopolymerized denture base polymers, all in the powder and liquid form, were chosen for this study (Table 1). The currently produced Superacryl and Duracryl are labeled cadmium free. Superacryl and Duracryl produced before 1994 contained cadmium (Cimpan et al., unpublished results). They were included in the present study because dentures made before 1994 from these materials can still be in use. The current versions will be referred to in this work as Superacryl 'New' (SN) and Duracryl 'New' (DN) and the previous versions as Superacryl (S) and Duracryl (D). All the denture base materials were within their shelf life. Vertex Rapid Simplified (VRS) was processed in boiling water for 20 min. Then the heat was turned off for 15 min and after that it was reheated to boil for an additional 20 min. For S and SN the following polymerization cycle was used: the temperature was raised to 60°C in the course of 30 min and then kept at 60°C for 60 min. After that the temperature was raised to 100°C in the course of 30 min and then kept for 30 min at 100°C. The autopolymerized materials were processed at 40°C for 15 min in a pressure pot under a pressure of 2.5 bar.

Preparation of test specimens and eluates

Acrylic specimens (50 mm diameter, 0.5 mm thickness) were fabricated under aseptic conditions in stainless steel molds according to the manufacturers' directions and the ISO recommendation (16). The specimen disks were used immediately after fabrication. Eluates were prepared following the ISO requirements (17) by placing the extraction medium and the specimens in Costar Petri dishes (60 mm diameter) (Cambridge, MA, USA) for 24 and 48 h at 37°C. Eagle's Minimum Essential Medium (EMEM) (BioWhittaker, Walkersville, MD, USA) with a 2% mix of penicillin/streptomycin/fungizone (PSF) (BioWhittaker) was used for extraction. Fetal bovine serum (FBS) and L-glutamine (BioWhittaker) were not added prior to exposure to the cells. The ratios between the mass of the test specimens and the volume of medium used for extraction were 0.2 g/ml, 0.4 g/ml, and 0.8 g/ml. For the negative control EMEM incubated under the same conditions was used. Eluates were stored at −20°C (5).

Cell culture

L929 murine fibroblasts (NCTC clone 929, the American Type Culture Collection, Manassas, VA, USA) were used in this study. Fibroblasts are relevant for an in vitro screening of the interfacial reaction because they are adherent cells and because the impairment of their metabolic functions may lead to a weaker or more permeable mucosa due to disturbances in the collagen formation (3). Moreover, such cells are exposed to denture bases when ulceration of the overlying epithelium occurs after denture placement (5). Cultures were routinely screened for mycoplasma infection (direct culture test). Cells were seeded at 400 cells/cm^2 in 75 cm^2 Costar polystyrene flasks in EMEM supplemented with 5% heat-inactivated (56°C, 30 min) FBS, 1% L-glutamine and 2% PSF, and kept in a controlled fully humidified atmosphere of 5% CO$_2$ and 95% air at 37°C. On day 5 or 6 the cultures were harvested by trypsinization and dispersed into new flasks. The cell line was used over a maximum of 30 passages to minimize changes that occur during prolonged culture. Only cells from cultures with a viability >95% (tested by exclusion of trypan blue 0.2%) were used in the experiments.

Colony-forming ability (clonogenicity)

The assay was essentially performed as described by Hay (18). Acrylic disks were placed on the bottom of Costar Petri dishes in 3 ml EMEM with the supplements mentioned above. The disks were pressed with tweezers against the bottom of the dishes. They remained attached to the bottom of the Petri dishes due to the adhesion created by the thin layer of EMEM, the surface of the specimen disk, and the bottom of the dish. The ratios between the mass of the test specimens and the volume of EMEM were 0.2 g/ml, 0.4 g/ml, and 0.8 g/ml. To obtain

the desired mass/volume ratio, specimens were placed either alone or on top of each other in the Petri dishes. Thus, in all experiments, cells were exposed to the surface of only one acrylic disk. L929 fibroblasts (100 cells per dish) were plated on the acrylic specimen facing the medium over a 10-day period. Cells seeded on the bottom of Petri dishes in EMEM plus supplements served as controls ($n = 6$). At the culture endpoints the medium was removed and spun down to pellet dead cells and debris. The supernatant was enriched with supplements and then transferred to new Petri dishes. The bottom of each dish was plated with 100 L929 cells over a 10-day period. Colonies were fixed with 2% glutaraldehyde and stained with Giemsa. Results were expressed as numbers of colonies in percentage of the controls. This assay was performed to assess whether the tested denture base polymers could impair the clonogenicity of L929 cells and if that was due to the leachables or to the direct contact with the cells.

Annexin V-FITC/Propidium iodide in situ staining of cells exposed to eluates

L929 cells were cultured in 24-well Costar plates at a density of 20,000 cells/cm^2 in 1.5 ml of eluate. Prior to addition to the cells eluates were enriched with the supplements mentioned above. Cells were incubated in the eluates for 24 and 48 h. L929 cells exposed to EMEM previously incubated under the same conditions as the eluates (24 h or 48 h at 37°C) provided the negative control. Cells treated for 24 and 48 h with 5000 U/ml human recombinant tumor necrosis factor alpha (TNF-α) (R&D Systems, Abingdon, UK) (19) or 10 µM etoposide (Amersham Int., Bucks, UK) (20) served as positive controls for apoptosis. In situ staining with Annexin V-FITC and PI (Apoptest® V-FITC Kit A-700, NeXins Research, Kattendijke, The Netherlands) was used for labeling apoptotic, secondary necrotic, and necrotic cells. At the culture endpoints plates were spun down 4 min at $200 \times g$, then the supernatant was removed and replaced with 245 µl of 10 times diluted binding buffer. Annexin V-FITC (0.25 µg/ml) and PI (2.5 µg/ml) were added and left at room temperature in the dark for 10 min. The cells were then rinsed gently with EMEM in order to remove unbound Annexin V-FITC and PI. Thereafter EMEM (200 µl) was added in each well in order to furnish nutrients to the cells. Stained cells were scrutinized by inverted fluorescent and scanning confocal microscope. A minimum of 300 test cells per sample was analyzed. Since the assay was done on live cells, in order to avoid false positive results, no more than three wells were analyzed at a time. Experiments were run three times in duplicate. Because the specimen disks stained green due to unspecific binding of Annexin V-FITC, this test could not be performed on L929 cells seeded directly on the disks.

Scanning confocal microscopy. The cells were examined using a Leica TCS NT confocal laser scanning microscope (Leica Lasertechnik GmbH, Heidelberg, Germany) at-

tached to an inverted (Leica DM IRBE) microscope. For optical sectioning 20× or 40× objectives were used and one section with a resolution of 512×512 pixels per channel was recorded for each specimen. In order to improve the quality of the slow scan mode, each section was recorded as an average of four pictures. FITC was excited with the 488 nm line of an Ar-Kr laser, whereas PI was excited with the 568 nm line. Fluorescence was obtained through a long pass filter (590 nm). The pinhole setting was optimized to gain maximum confocal quality. Cellular morphology was combined with the confocal images (the Annexin V-FITC labeled cells stained green using FITC filter optics and the nuclei of the PI labeled cells stained red using TRITC filter optics) using a transmission detector and Hoffman optics.

DNA stainability with propidium iodide—quantification of apoptosis based on the 'sub-G1' peak

To determine whether the tested polymers induced apoptosis and if that was due to leachables or to direct contact with the cells the following test was performed. Specimen disks were placed on the bottom of Petri dishes in EMEM with supplements. The ratios between the mass of the test specimens and the volume of EMEM were 0.2 g/ml, 0.4 g/ml, and 0.8 g/ml. L929 cells (20,000 cells/cm^2) were plated on the acrylic specimen facing the medium for 24 and 48 h. Cells seeded on the bottom of Petri dishes in EMEM plus supplements served as controls. At the culture endpoints the medium from each dish was removed, spun down, and the supernatant was transferred to new Petri dishes. Each Petri dish containing 3 ml of supernatant was plated with 20,000 L929 cells/cm^2 for 24 and 48 h. At the culture endpoints of each type of assay (i.e. eluates and direct contact) adherent L929 cells were collected by trypsinization and pooled together with cells that lost attachment (i.e. 'floating cells'). The cells were pelleted, washed, and then prepared for DNA quantification as described by Cimpan et al. (6) and Coligan et al. (21). After staining with PI, the cells were analyzed by flow cytometry (Coulter Epics XL-MCL, Coulter Corporation, Harpende, UK) using a 488 nm laser line for excitation. Red fluorescence (>600 nm) was measured for 30,000 cells per sample at forward light scatter. The linear red fluorescence histograms with a 256-channel resolution were analyzed. Only objects with a fractional DNA index greater than 10% of that of intact G1 cells were considered (14). At least three individual experiments were made, each experiment performed in duplicate. Data analysis was performed with the Coulter Epics XL software version 1.5 (Coulter Corporation, Harpende, UK) and with WinMDI 2.7 (22).

Electron microscopy

The procedure was performed essentially as described by Cimpan et al. (6). Cells exposed to eluates that remained adherent to the bottom of the Petri dishes were

trypsinized, pooled together with the cells floating in the supernatant EMEM, and spun down. The medium from the Petri dishes in which L929 cells were seeded directly on specimen disks, was aspirated and floating cells were spun down. The cell pellets and the adherent cells on the acrylic disks were fixed separately in glutaraldehyde (1.5% v/v) in 0.1M Na-cacodylate buffer, pH of 7.4 for 30 min at room temperature, then rinsed, post-fixed in 1.0% (w/v) OsO_4 in 0.1M Na-cacodylate buffer, pH of 7.4 for 1 h at 4°C, dehydrated and embedded in Agar 100 resin. Ultrathin sections were contrasted with 2% uranyl acetate and lead citrate and examined under a JEOL 100CX electron microscope.

Statistical analysis

The sign test was used for analyzing the results from the clonogenicity test. Statistical analysis based on the mixed effect model (23) was performed on the percentages of apoptotic, secondary necrotic, and necrotic L929 cells, considering P-values less than 5% as significant. The control group was set as reference. The day of the cell culture was entered as a random factor to control for possible changes in the cell culture over time, whereas the material, the eluate concentration (i.e. mass/volume ratio), the time of exposure, and the method were implemented as fixed factors. Data were analyzed and displayed on a log scale because log-transformed data fitted a normal distribution. The percentages of necrotic, secondary necrotic and apoptotic cells were expressed as geometric means with 95% confidence limits. The experimental standard uncertainty was evaluated based on the standard deviation of the mean as: $U = SD/\sqrt{n}$ (24).

Results

Clonogenicity

Colonies were formed on all VRS, SN, and VSC disks and eluates. Colonies were found in 0.2 g/ml eluates from Q, D, and DN and in all the eluates from S. No colonies were formed on S, Q, D, and DN disks regardless of the ratios between the mass of the disks and the volume of EMEM (Fig. 1A–C).

Annexin V-FITC in situ labeling and DNA quantification

As visualized by confocal microscopy, early apoptotic cells stained only green with Annexin V-FITC (Fig. 2B, D). Secondary necrotic cells (i.e. in later stages of apoptosis) and necrotic cells stained green with Annexin V-FITC and their nuclei stained red with PI. Cells stained green and red were considered secondary necrotic if their volume was reduced (Fig. 2B–D) and necrotic if their volume was increased (Fig. 2C) compared to viable cells.

In the DNA histograms of PI-stained L929 cells (Fig. 3A–C) the hypodiploid cells (i.e. apoptotic) were placed in
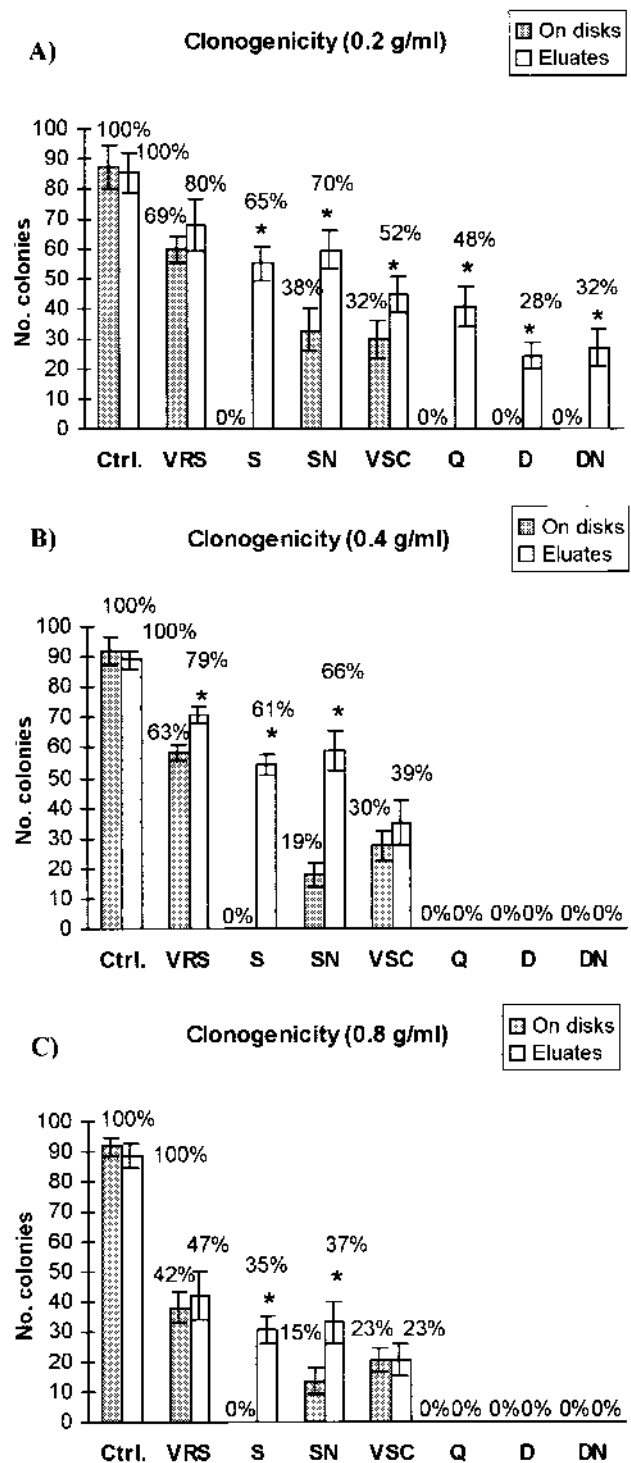

Fig. 1. Number of colonies formed by L929 cells on resin disks and their eluates at (A) 0.2 g/ml, (B) 0.4 g/ml and (C) 0.8 g/ml. 100 cells were seeded over a 10-day period on each resin disk and in each eluate. The bottom of Costar Petri dishes served as control ($n = 6$). The percentage above each bar represents the number of colonies expressed as percentage of the control. Significant differences between disks and eluates of each material are marked * ($P < 0.05$); sign test.
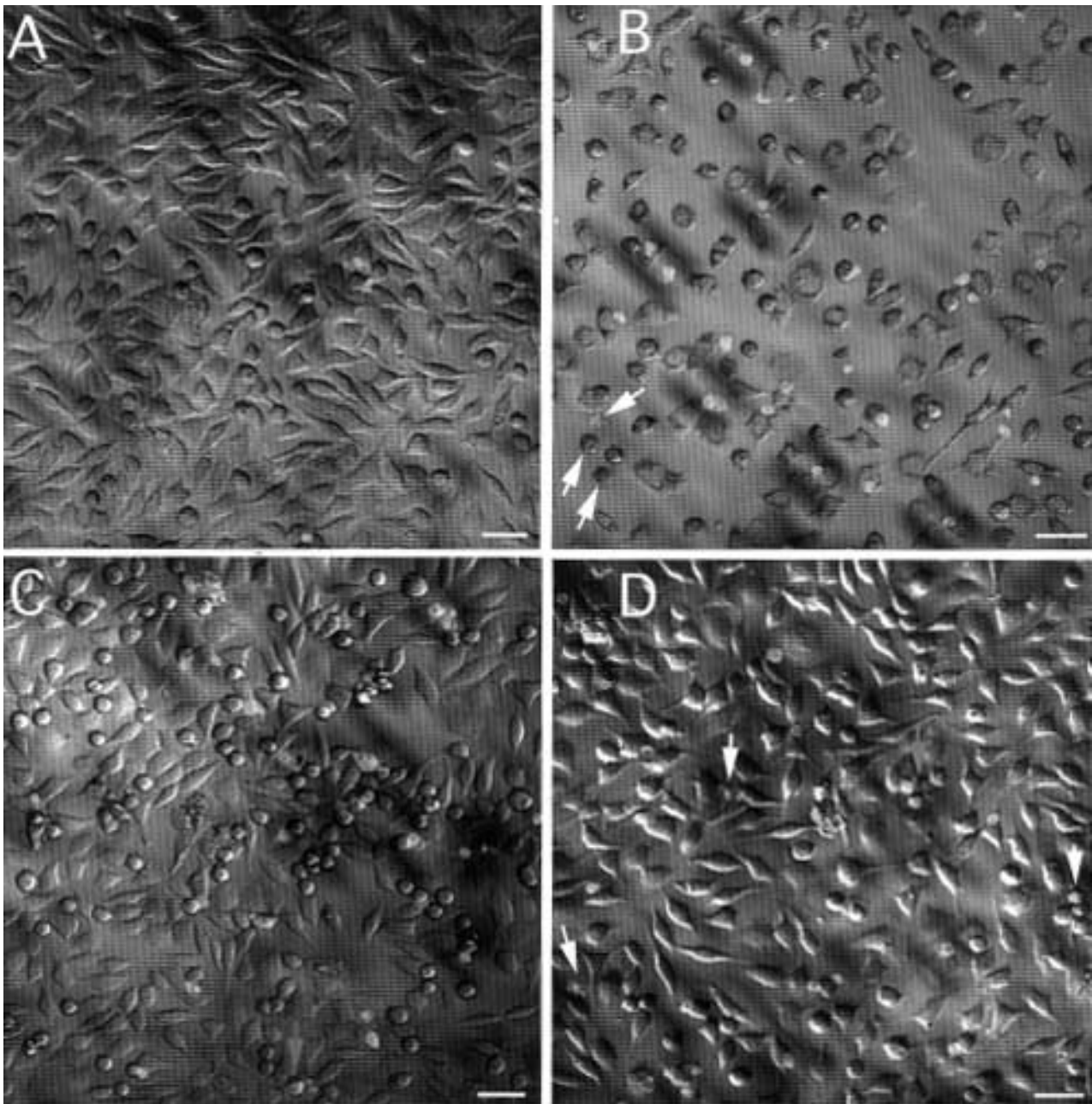
Fig. 2. Effects of eluates on in situ staining of L929 cells with Annexin V-FITC and PI: (A) untreated cells and cells exposed for 24 h to: (B) 10 μM etoposide, (C) 48-h VRS eluate of 0.8 g/ml, (D) 48-h D eluate of 0.8 g/ml. The cells were examined with a Leica TCS NT confocal laser scanning microscope attached to an inverted microscope (20× objective). Four distinct phenotypes become distinguishable: (i) viable cells—unstained, (ii) apoptotic cells—stained only green (white arrows), (iii) secondary necrotic cells—shrunken cells stained green and red (purple arrows), and (iv) necrotic cells—swollen cells stained green and red (blue arrows). Bars = 30 μm.

a separate 'sub-G1' peak (M1) to the left of the main G0/G1 peak. A significantly higher proportion of cells was found in the 'sub-G1' peak when L929 fibroblasts were seeded directly on disks than when seeded in eluates of VRS, S, and DN (all *P* values <0.05).

The percentage of dead cells increased with concentration (Fig. 4A, B), but not with time (Fig. 5A, B). Table 2

gives an overview of the levels of apoptosis, secondary necrosis, and necrosis induced by the eluates of the tested denture base polymers. The autopolymerized Q, D, and DN induced higher percentages of apoptosis, secondary necrosis, and necrosis than the heat-polymerized polymers. D and DN induced the highest percentages of apoptosis and necrosis. Of the autopolymerized polymers only VSC
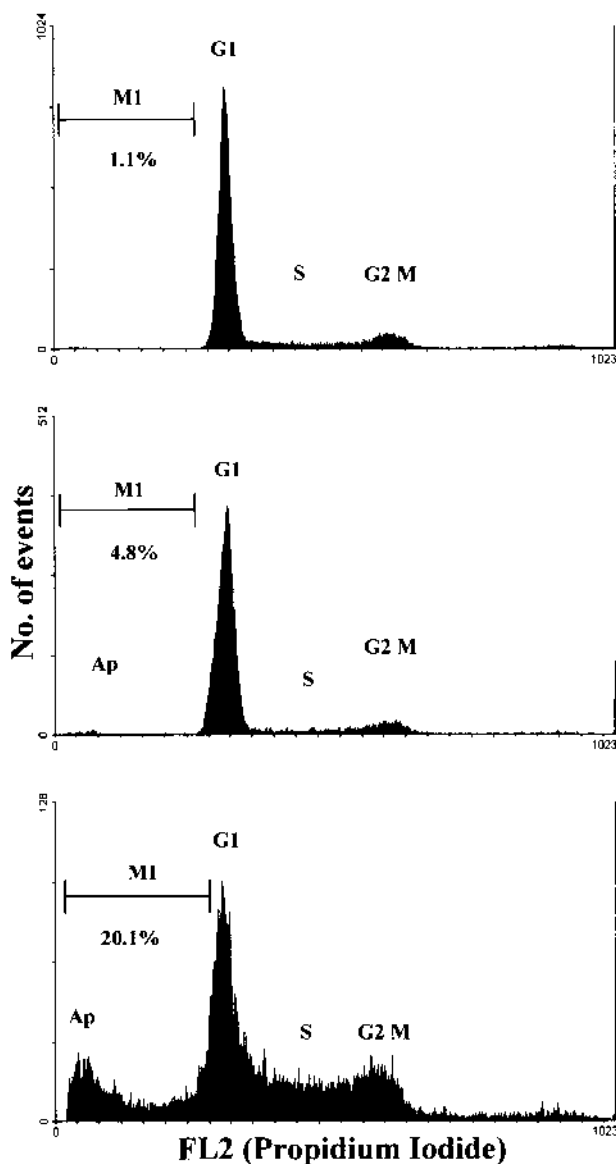
Fig. 3. Apoptosis induced by eluates—measured by DNA quantification. DNA fluorescence histograms of PI-stained L929 cells: (A) untreated cells (B) cells treated for 48 h with a 48-h VRS eluate of 0.8 g/ml (C) cells treated for 48 h with a 48-h D eluate of 0.8 g/ml (note the presence of a 'sub-G1' peak (Ap) given by apoptotic cells). The position of the apoptotic cells (Ap) and the different phases of the cell cycle (G1, S and G2/M) are marked. Marker M1 was used to calculate the percentage of cells undergoing apoptosis.

produced lower overall values for apoptosis than a heat-polymerized polymer, namely S. The highest levels of cell death were induced by the 0.8 g/ml eluates and disks of the acrylic polymers. All denture base materials decreased the viability of L929 cells when collected after the two time intervals. No significant difference was found between the two time intervals ($P = 0.399$).

Annexin V-FITC/PI staining and DNA quantification provided concordant results regarding apoptosis ($P =$

0.074). Based on the evaluation of the standard uncertainty (u_s for apoptosis = 0.53%, u_s for secondary necrosis = 0.25% and u_s for necrosis = 0.38%), we considered that the reliability of the measurements was high.

Electron microscopy

The L929 cells exposed for 24 h to 24-h eluates (0.8 g/ml) of VRS and D rounded up, their volume decreased and cytoplasm condensed. The shape of the nuclei became more irregular and a redistribution of the chromatin could be seen (Fig. 6B, C). The inner nuclear membrane remained close to the nucleosol and the nucleoli appeared disorganized. Small vacuoles were seen in the cytoplasm and the cytoskeleton was altered (Fig. 6C). The mitochondria tended to gather in one part of the cell (Fig. 6C) and seemed to be slightly condensed (Fig. 6B, C). In cells treated with VRS eluates microvilli disappeared and blebbing and cell fragmentation were often seen (Fig. 6B). Some of the L929 cells that were seeded on VRS and D remained adherent to the disks (Fig. 7C, F) while others detached (Fig. 7B, D, E). The nuclei of the floating cells often became more irregular in shape, and redistribution of the chromatin and disorganized nucleoli were occasionally seen (Fig. 7B, D). A few large, probably autophagic vacuoles were detected (Fig. 7B–D). A minor cluster of cells treated with D was associated with characteristic signs of necrosis: cell swelling, decondensation of chromatin, swelling of mitochondria and endoplasmic reticulum, and disruption of cell membranes (Fig. 7E). Mitochondria in untreated L929 fibroblasts were radially distributed around the nucleus and had round or oval shape with well-defined cristae (Fig. 7A). Blebbing or cell fragmentation were not observed. Morphological changes in TNF-α treated L929 fibroblasts (Fig. 8) were similar to those observed in L929 cells that subsequently detached from VRS and D disks (Fig. 7B, D).

Discussion

It is important to differentiate between apoptosis and necrosis when evaluating the cytopathogenic effects of biomaterials because apoptosis and necrosis have different biological significance. Apoptosis maintains the homeostasis by eliminating damaged, unwanted cells in an orderly and clean fashion, which minimizes tissue injury and scar formation. Apoptosis is a gene-regulated process and therefore can be selectively modulated, offering the possibility to obtain the desired reaction at the tissue/material interface. Necrosis is an accidental process, which induces inflammation and injuries to the surrounding tissues. Therefore, more severe tissue reactions may occur if the biomaterial induces mainly necrosis.

The comparison of the ability of L929 fibroblasts to form colonies on denture base acrylic disks and in their eluates allowed a simple screening to assess whether the deleterious effects were caused by toxic leachables or by
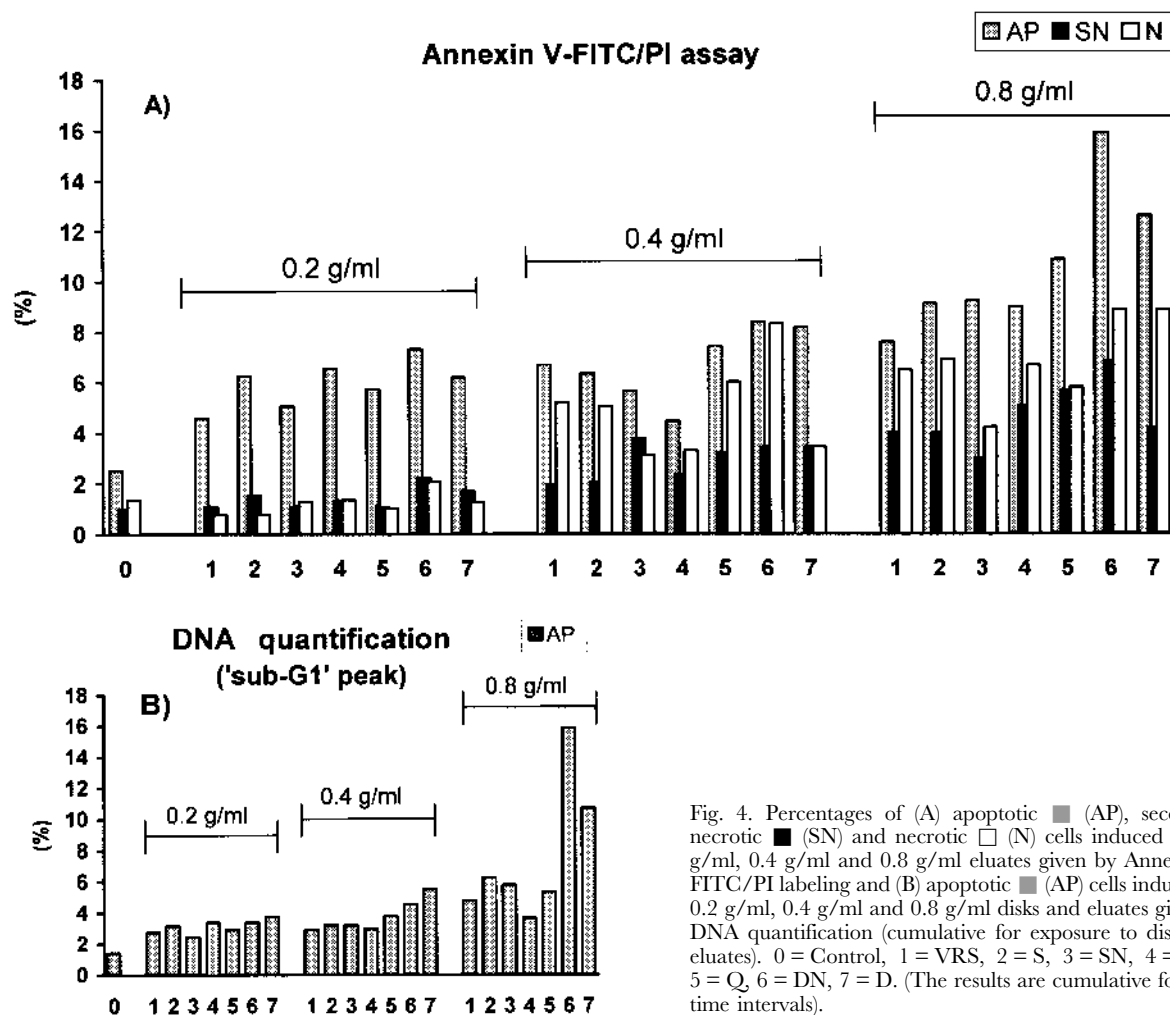
Annexin V-FITC/PI assay

DNA quantification
('sub-G1' peak)

Fig. 4. Percentages of (A) apoptotic ▨ (AP), secondary necrotic ■ (SN) and necrotic □ (N) cells induced by 0.2 g/ml, 0.4 g/ml and 0.8 g/ml eluates given by Annexin V-FITC/PI labeling and (B) apoptotic ■ (AP) cells induced by 0.2 g/ml, 0.4 g/ml and 0.8 g/ml disks and eluates given by DNA quantification (cumulative for exposure to disks and eluates). 0 = Control, 1 = VRS, 2 = S, 3 = SN, 4 = VSC, 5 = Q, 6 = DN, 7 = D. (The results are cumulative for both time intervals).

the surface characteristics of the denture base polymers. The response to eluates demonstrated that, except for VSC, the autopolymerized polymers were more cytotoxic than the heat-polymerized. Colonies were not formed on the disks of S, Q, D, and DN regardless of concentration, but they did form their 0.2 g/ml eluates. This implies that the surface characteristics (e.g. hydrophilicity, charges, surface energy, roughness, and morphology) of the S, Q, D, and DN disks did not allow the L929 fibroblasts to attach and form colonies. Significant differences were seen between brands belonging to the same type of denture base materials. Thus, S was the only heat-polymerized polymer on which colonies were not formed, while VSC was the only autopolymerized acrylic on which colonies were formed. To explain these differences more information is needed about the chemical composition and the surface properties of each brand.

Clonogenic survival assays are usually focused on the surviving colonies and therefore, the fate of the cells that do not form colonies may pass unnoticed. In a recent study it was demonstrated that the loss of the clonogenic potential is a measure of the commitment to cell death and that it can precede the key biochemical or morphological features of apoptosis (25). The results obtained in the Annexin V-FITC/PI labeling test indicate that L929 cells die mainly by apoptosis and in a lower proportion by necrosis. In our study, clonogenicity impairment is in accordance with the results for apoptosis, indicating that this type of test could be used as a preliminary screening of the cellular viability and commitment to death. This type of in vitro screening is a useful starting point for investigating the interactions between cells and the surface of a biomaterial.

There seem to be several varieties of apoptosis and different cell types may follow different rules (9). L929 cells, like other fibroblasts, do not always display the classic profile of apoptosis (19, 20). One feature that is frequently missing in apoptotic L929 cells is endonucleolytic DNA fragmentation (20, 26, 27). Therefore, we chose not to use agarose gel electrophoresis or the terminal deoxynucleotidyl transferase nick end labeling (TUNEL) assay for the detection of apoptosis. In the L929 cells exposed to
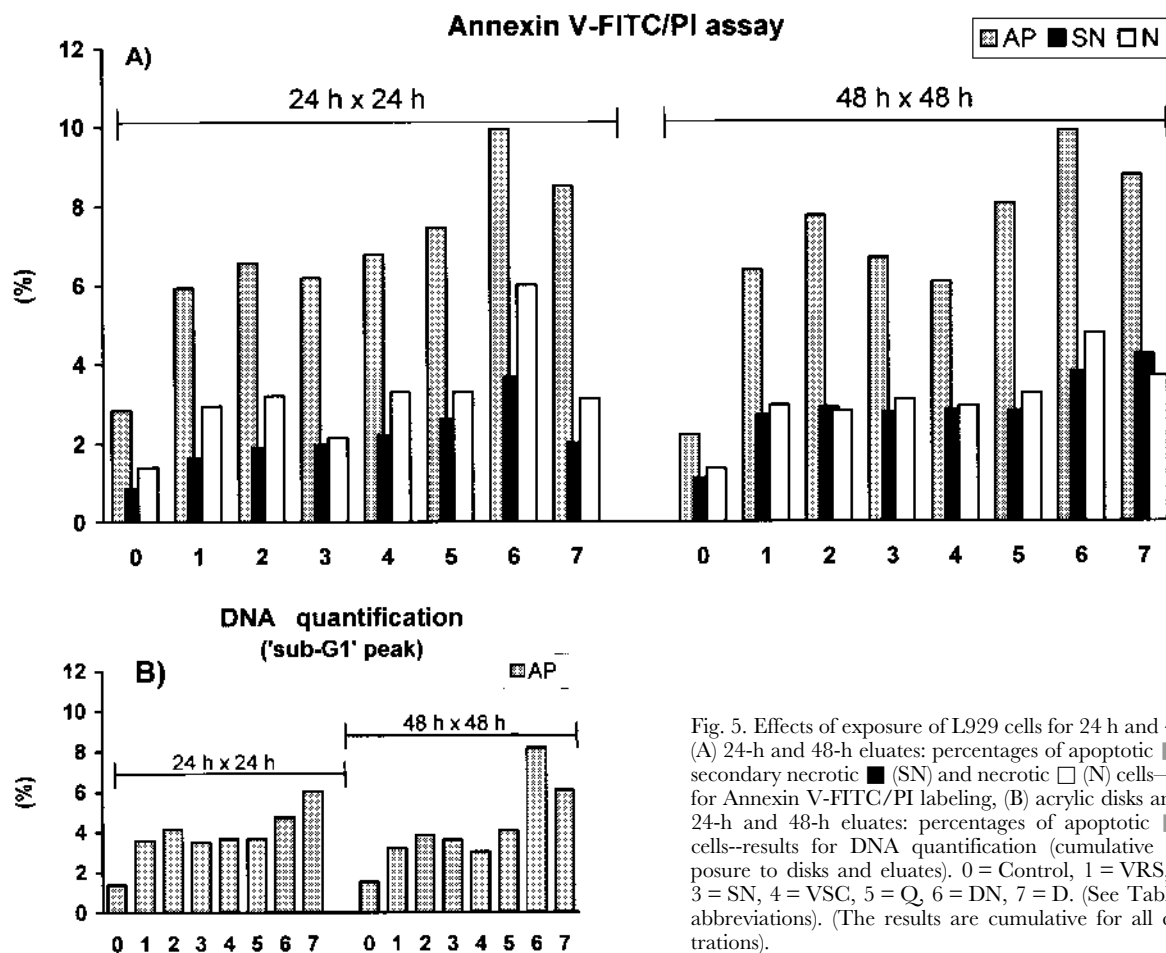
Fig. 5. Effects of exposure of L929 cells for 24 h and 48 h to: (A) 24-h and 48-h eluates: percentages of apoptotic ▨ (AP), secondary necrotic ■ (SN) and necrotic □ (N) cells—results for Annexin V-FITC/PI labeling, (B) acrylic disks and their 24-h and 48-h eluates: percentages of apoptotic ▨ (AP) cells--results for DNA quantification (cumulative for exposure to disks and eluates). 0 = Control, 1 = VRS, 2 = S, 3 = SN, 4 = VSC, 5 = Q, 6 = DN, 7 = D. (See Table 1 for abbreviations). (The results are cumulative for all concentrations).

denture polymers, clumping and redistribution of the chromatin together with cell shrinkage, and for the cells exposed to VRS blebbing, could be seen. The vesicularization present in the L929 cells treated with eluates and more pronounced in those seeded directly on polymer disks, has been seen previously in advanced stages of apoptosis in fibroblasts (28). The morphological changes seen in cells seeded directly on the acrylic disks were more

dramatic than in cells seeded in eluates, indicating the impact that the surface properties have on the morphology of L929 fibroblasts. Since these cells display an atypical apoptotic morphotype, two apoptosis inducers were used in the positive controls (i.e. TNF-α and etoposide). The morphological features of the cells exposed to TNF-α matched those described by Fady et al. (19).

The presence of apoptosis detected by electron micro-

Table 1. Denture base acrylic polymers used in the investigation

Material	Batch no.		Powder/Liquid ratio	Manufacturer
	Powder	Liquid		
Heat-polymerized				
1. Vertex RS (VRS)	8910254	1680671	3:1 (vol.)	Dentimex BV, The Netherlands
2. Superacryl (S)	4010890	4601276	2:1 (g)	Spofa Dental-Praha, Czech Republic
3. Superacryl 'New' (SN)	4010694	4030694	2:1 (g)	Spofa Dental-Praha, Czech Republic
Autopolymerized				
4. Vertex SC (VSC)	9402224	GN261L07	3:1 (vol.)	Dentimex BV, The Netherlands
5. Quick SR 3/60 Type 10 (Q)	529895	442768	3:1 (vol.)	Ivoclar AG, Liechtenstein
6. Duracryl (D)	4020394	4010594	3:1 (vol.)	Spofa Dental-Praha, Czech Republic
7. Duracryl 'New' (DN)	97403	104731	3:1 (vol.)	Spofa Dental-Praha, Czech Republic
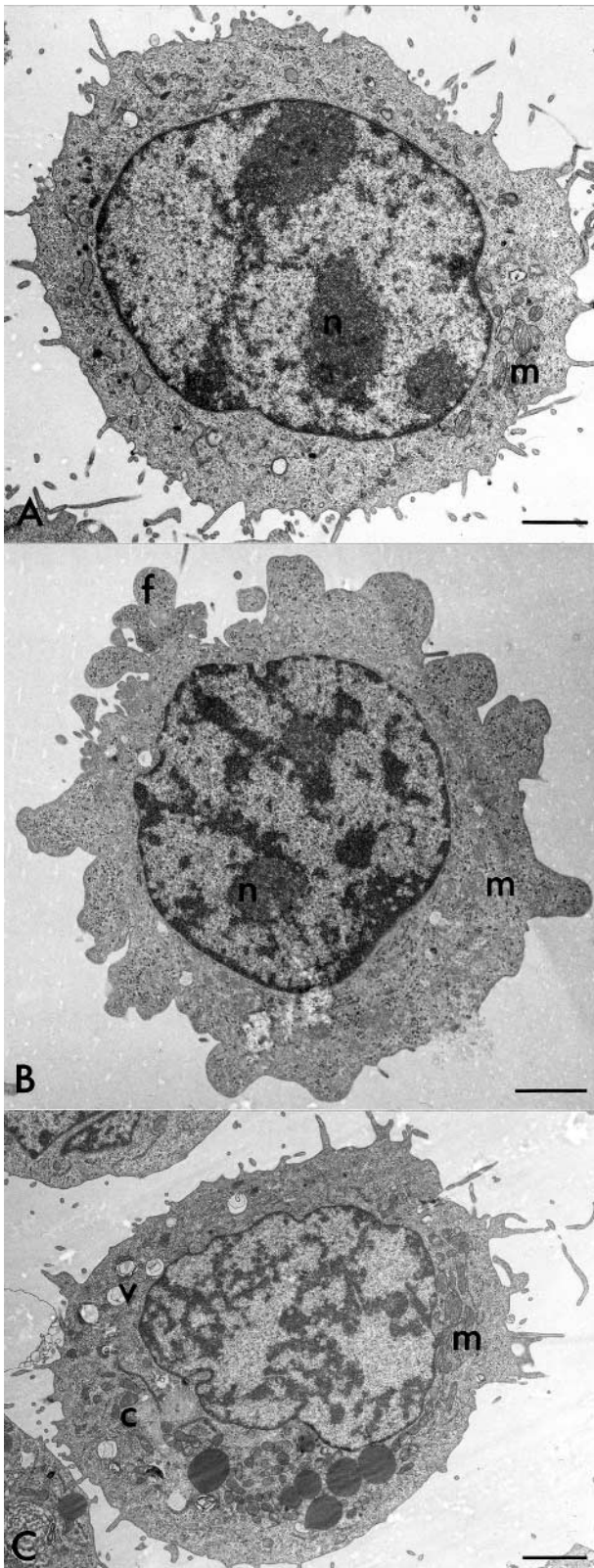
scopy was confirmed by Annexin V-FITC labeling and by the presence of the 'sub G1' peak. The presence of a 'sub-G1' peak in apoptotic L929 cells has been detected in prior studies (20, 26, 29). The score for apoptosis was generally lower in the DNA quantification assay than in the PS detection test because apoptotic cells in the S and G2/M phases do not appear in the 'sub-G1' shoulder. A general trend was observed for eluates from all polymers, namely, a steep increase of the percentage of necrotic cells at 0.4 g/ml and 0.8 g/ml. The number of cells in the early apoptotic stage increased moderately at these concentrations, while the number of cells in the late stage of apoptosis (i.e. secondary necrotic) increased more steeply. However, early apoptotic together with late apoptotic cells outnumbered necrotic cells at all concentrations. Taken together, these findings suggest that more severe tissue reactions may appear at higher concentrations. If such high concentrations could be reached in vivo remains to be elucidated.

The stronger cytopathogenic effect of the direct contact on L929 cells in all the tests could be explained by the addition of the effect of the surface properties of the denture polymers to the toxic effect of their eluates. Another explanation could be that the toxic effect of the leachables is stronger when cells are exposed to them during their release. The cytotoxic potential of the eluates may diminish in time due to progressive degradation or complexion of toxic leachables with other chemicals in the medium (5). A relevant question would be why was the effect of S, Q, D, and DN disks more dramatic in the clonogenicity test than in the DNA quantification assay. The answer may be that in the colony forming assay cells were plated at a much lower cell density than in the DNA quantification test and thus the growth inducing effects from neighboring cells were prevented. Another explanation could reside in the much longer duration of cell exposure to the polymers in the clonogenicity test.

A relatively low cell density (20,000 cells/cm^2) was chosen for the Annexin V-FITC, DNA quantification, and electron microscopy assays because a monolayer culture is most reproducible and homogeneous when it is in the growth phase, before it reaches confluence (30). Although higher cell densities more closely mimic in vivo conditions, cell monolayers are more fragile at high densities (31).

Determination of the surface area of the specimens was difficult and gave higher inaccuracy than determination of

Fig. 6. Ultrastructure of L929 cells grown for 24 h in EMEM standard medium (A) and in 24-h eluates of 0.8 g/ml from VRS (B) and D (C). L929 cells exposed to VRS and D rounded up and the shape of their nuclei became slightly more irregular. Redistribution of the chromatin was observed (C). In the cytoplasm small vacuoles and clustering of actin filaments were seen (C). Mitochondria were condensed and tended to gather together (C). Blebbing, cell fragmentation and disappearance of microvilli were observed in cells exposed to VRS eluates (B). Abbreviations: c = cytoskeleton, f = cellular fragments, m = mitochondria, *n* = nucleolus, v = vacuoles. Bars = 2 μm.
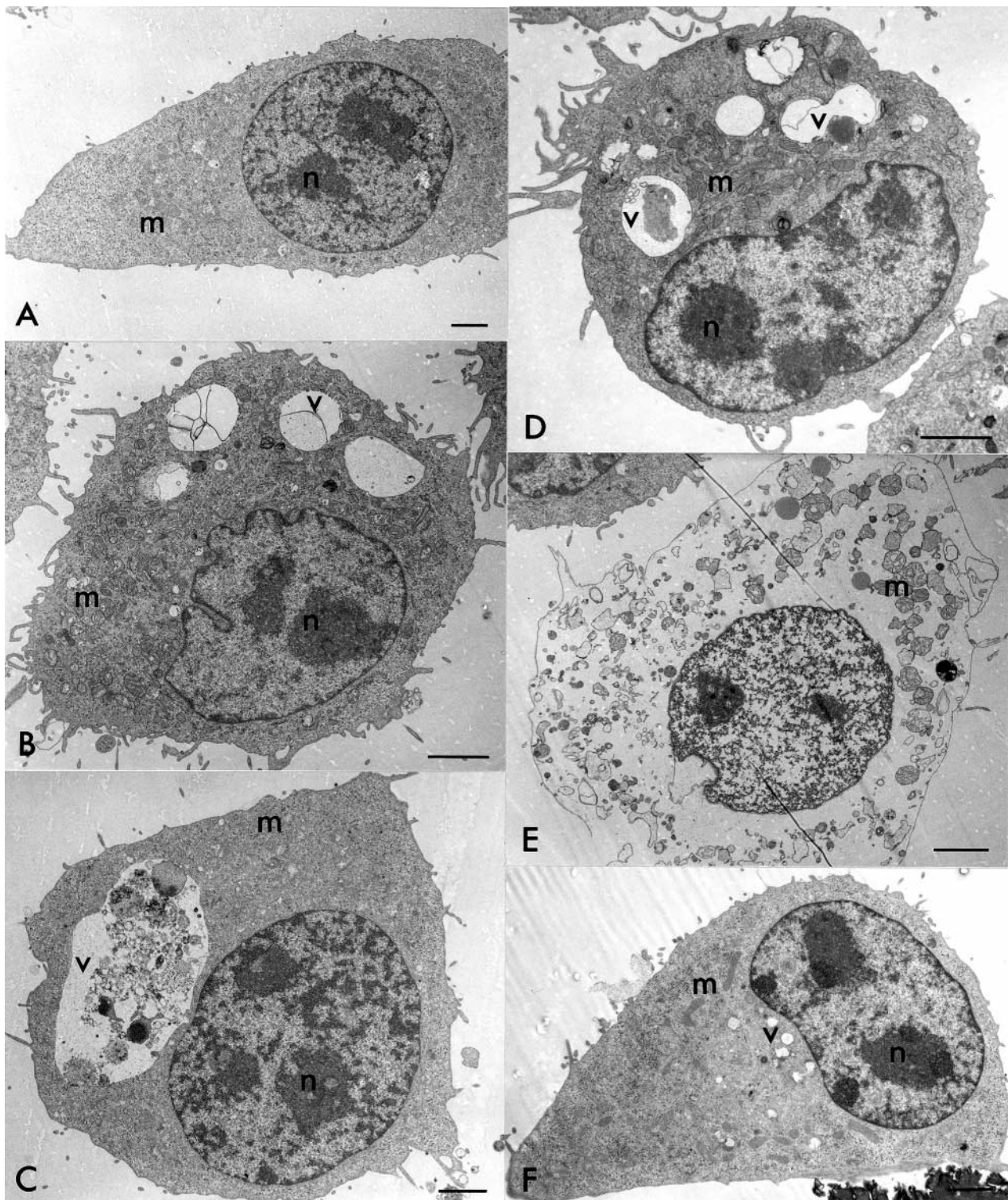
Fig. 7. Electron micrographs of L929 cells seeded for 24 h on the bottom of Petri dishes in EMEM standard medium (A) and directly on disks (0.4 g/ml) of VRS (B, C) and D (D, E, F). Cells that remained attached to the VRS (C) and D (F) disks were shrunken and tended to round up. The cells that detached from VRS (B) and D (D) disks (i.e. "floating cells") had nuclei with a more irregular shape and contained large vacuoles in the cytoplasm. Necrotic cell death (E) was characterized by cell and mitochondrial swelling and decondensation of chromatin. Abbreviations: m = mitochondria, *n* = nucleolus, v = vacuoles. Bars = 2 μm.
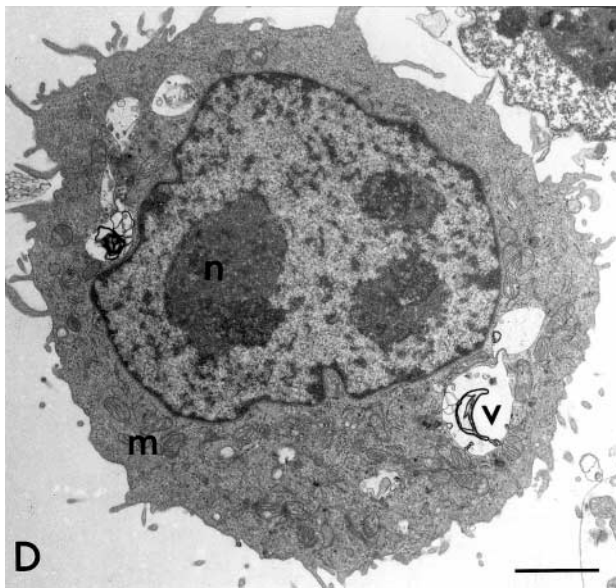
Fig. 8. Ultrastructure of L929 cells treated with TNF-α (5000 U/ml, 24 h) -- positive control for apoptosis. The cells shrunk, rounded up, and large vacuoles appeared in the cytoplasm. Abbreviations: m = mitochondria, *n* = nucleus, v = vacuoles. Bar = 2 μm.

their mass. Therefore, we chose to use the ratio between the mass of the specimens and the volume of the extraction medium, as recommended by the ISO (17).

Eluates of denture base polymers have been proven to produce alterations in several classes of cell lipids (4). Eluates contain often benzoyl peroxide (BPO), commonly used as a polymerization initiator in denture base polymers (1). Peroxidation of cellular lipids by BPO may be a major mechanism of toxicity (32). Peroxides can produce activation of phospholipase A2, uncoupling of oxidative phosphorylation with concomitant effects on ATP production, and alterations of calcium homeostasis (33). These findings might explain our observation that morphological modifications in L929 cells seeded on VRS and D disks were similar to those induced by TNF-α since its cytotoxicity is mediated, at least in part, by oxidative stress and phospholipase A2 activation (34). In oxidative stress, which affects many cellular components and structures, the cytotoxic effects are nonspecific and the mechanisms leading to cell death are poorly understood (35). This could explain the atypical morphology of the L929 cells in the present study. Other compounds that may be responsible for inducing apoptosis and necrosis are methyl methacrylate (MMA) and the products resulted from its oxidation and hydrolysis: formaldehyde and methacrylic acid respectively. Unreacted MMA leaches out from denture base resins and is able to block the electron transport and to uncouple oxidative phosphorylation in the mitochondria (36).

It has been shown that there is more residual MMA in the autopolymerized than in the heat-cured polymers (37, 38). In addition, it has been found that a significantly

higher amount of MMA is released from autopolymerized PMMA than from heat-cured PMMA (38). In the case of BPO, heating hastens its breakdown and therefore its effects when leaching out of heat-cured materials would be less pronounced (39). These previous findings may explain why three of the autopolymerized polymers had stronger cytopathogenic effects than the heat-polymerized polymers. However, the polymerization conditions alone are not enough to explain the effect of each material. Thus, VSC, an autopolymerized polymer, had a lower cytopathogenic effect than the heat-cured S. Although cured for a much shorter time than S and SN, the heat-polymerized VRS had the lowest death-inducing potential. To determine the causes for these differences, the chemical composition and the leachable compounds of each brand should be identified and the apoptogenic and necrogenic potential of each component should be assessed.

This study provides evidence that two distinct modes of cell death—apoptosis and necrosis—are involved in the cytopathogenic effects induced by PMMA-based denture base polymers on L929 murine fibroblasts. Furthermore, apoptosis was demonstrated to be the major mode of cell death. The tested denture base polymers augmented the cell death and decreased the clonogenicity of L929 cells in the following rank order of potency: Duracryl > Duracryl 'New' > Quick SR > Superacryl > Vertex SC > Superacryl 'New' > Vertex RS. The present data corroborate earlier results obtained with eluates from the same denture base polymers in the U-937 human monoblastoid cell line (6). In general, the deleterious effects were stronger when cells were plated directly on the polymer disks than in the eluates. Although the clinical significance of our findings remains to be elucidated, the information presented here may contribute to a better understanding of the mechanisms involved in the interactions between cells and a biomaterial surface—a prerequisite for the rational development of medical devices with optimal biocompatibility.

References

1. Annusavice KJ. Denture base resins: technical considerations and processing techniques. In: Annusavice KJ, editor. Phillips' science of dental materials. 10th ed. Philadelphia: W. B. Saunders; 1996. p. 237–71.
2. Hensten-Pettersen A, Wictorin L. The cytotoxic effect of denture base polymers. Acta Odontol Scand 1981;39:101–6.
3. Lefebvre CA, Schuster GS, Marr JC, Knoernschild KL. The effect of pH on the cytotoxicity of eluates from denture base resins. Int J Prosthodont 1995;8:122–8.
4. Schuster GS, Lefebvre CA, Dirksen TR, Knoernschild KL,

Caughman GB. Relationships between denture base resin cytotoxicity and cell lipid metabolism. Int J Prosthodont 1995; 8:580–6.

5. Sheridan PJ, Koka S, Ewoldsen NO, Lefebvre CA, Lavin MT. Cytotoxicity of denture base resins. Int J Prosthodont 1997;10: 73–7.

6. Cimpan MR, Cressey LI, Skaug N, Halstensen A, Lie SA, Gjertsen BT, Matre R. Patterns of cell death induced by eluates from denture base acrylic resins in U-937 human monoblastoid cells. Eur J Oral Sci 2000;108:59–69.

7. Ratner BD. New ideas in biomaterials science—a path to engineered biomaterials. J Biomed Med Res 1993;27:837–50.

8. Kerr JFR, Wyllie AH, Currie AR. A basic biological phenomenon with wide-ranging implications in tissue kinetics. Br J Cancer 1972;26:239–57.

9. Majno G, Joris I. Apoptosis, oncosis and necrosis: an overview of cell death. Am J Pathol 1995;146:3–15.

10. Trump BF, Berezesky IK, Chang SH, Phelps PC. The pathways of cell death: oncosis, apoptosis, and necrosis. Toxicol Pathol 1997;25:82–8.

11. Clarke PG. Developmental cell death: morphological diversity and multiple mechanisms. Anat Embryol 1990;181:195–213.

12. Gjertsen BT, Cressey LI, Ruchaud S, Houge G, Lanotte M, Døskeland SO. Multiple apoptotic death types triggered through activation of separate pathways by cAMP and inhibitors of protein phosphatases in one (IPC leukaemia) cell line. J Cell Sci 1994;107:3363–77.

13. Koopman G, Reutelingsperger CP, Kuijten GAM, Keehnen RMJ, Pals ST, Van Oers MHJ. Annexin V for flow cytometric detection of phosphatidylserine expression on B cells undergoing apoptosis. Blood 1994;84:1415–20.

14. Darzynkiewicz Z, Juan G, Li X, Gorczyca W, Murakami T, Traganos F. Cytometry in cell necrobiology: Analysis of apoptosis and accidental cell death (necrosis). Cytometry 1997; 27:1–20.

15. Wilson AP. Cytotoxicity and viability assays. In: Freshney RI, editor. Animal cell culture: a practical approach. 2nd ed. New York: Oxford University Press Inc.; 1992. p. 263–305.

16. [ISO] International Organization for Standardization Dentistry—Denture base polymers. 1567:1988 (E). Clause 7.3.2. 2nd ed. Geneva: ISO; 1988. p. 1–9.

17. [ISO] International Organization for Standardization. Biological evaluation of medical device—Part 5: Tests for cytotoxicity: in vitro methods. 10993–5:1992 (E). 1st ed. Geneva: ISO; 1992. p. 1–7.

18. Hay RJ. Cell line preservation and characterization. In: Freshney RI, editor. Animal cell culture: a practical approach. 2nd ed. New York: Oxford University Press Inc.; 1992. p. 101–4.

19. Fady C, Gardner A, Jacoby F, Briskin K, Tu Y, Schmid I, Lichtenstein E. Atypical apoptotic cell death induced in L929 targets by exposure to tumor necrosis factor. J Interferon Cytokine Res 1995;15:71–80.

20. Bonelli G, Sacchi MC, Barbiero G, Duranti F, Goglio G, Verdun di Cantogno L, et al. Apoptosis of L929 cells by etoposide: a quantitative and kinetic approach. Exp Cell Res 1996;228:292–305.

21. Coligan JE, Kruisbeek AM, Margulies DH, Shevach EM, Strober W, Coico R. Flow cytometry for DNA analysis. In: Current protocols in immunology; 1995. p. 5.7.1–6.

22. Trotter J. WinMDI 2.7. Build #16 software (PC/Windows). Scripps Research Institute, 1998. Available from URL: http://www.uwcm.ac.uk/uwcm/hg/hoy/software.html.

23. Norusis MJ. SPSS base 8.0: How to obtain a factorial analysis of variance. In: Guide to data analysis. Prentice-Hall Inc., New Jersey, SPSS Inc; 1998. p. 301–8.

24. [BIPM] Bureau International des Poids et Mesures. Guide to the expression of uncertainty in measurement. 1st ed., Geneva: ISO; 1995. p. 9–18.

25. Brunet CL, Gunby RH, Benson RSP, Hickman JA, Watson AJM, Brady G. Commitment to cell death measured by loss of clonogenicity is separable from the appearance of apoptotic markers. Cell Death Differ 1998;5:107–15.

26. Barbiero G, Duranti F, Goglio G, Verdun di Cantogno L, Martinis O, Sacchi C, et al. Apoptosis models in HL-60 and L929 cells. Fundam Clin Immunol 1995;3:88–9.

27. Sculze-Osthoff K, Walczak H, Dröge W, Krammer PH. Cell nucleus and DNA fragmentation are not required for apoptosis. J Cell Biol 1994;127:15–20.

28. Evan GI, Wyllie AW, Gilbert CS, Littlewood TD, Land H, Brooks M, et al. Induction of apoptosis in fibroblasts by c-myc protein. Cell 1992;69:119–28.

29. Sanchez-Alcazar J, Ruiz-Cabello J, Hernandez-Muñoz I, Pobre PS, de la Torre P, Siles-Rivas E, et al. Tumor necrosis factor-α increases ATP content in metabolically inhibited L929 cells preceding cell death. J Biol Chem 1997;272:30167–77.

30. Freshney RI. Quantitation and experimental design. In: Freshney RI, editor. Culture of animal cells: a manual of basic technique. 2nd ed. New York: Wylie-Liss Inc.; 1987. p. 227–44.

31. Wataha JC, Hanks CT, Craig RG. The effect of cell monolayer density on the cytotoxicity of metal ions which are released from dental alloys. Dent Mater 1993;9:172–6.

32. Terakado M, Yamazaki M, Tsujimoto Y, Kawasima T, Nagashima K, Ogawa J, et al. Lipid peroxidation as a possible cause of benzoyl peroxide toxicity in rabbit dental pulp—a microsomal lipid peroxidation in vitro. J Dent Res 1984;63: 901–5.

33. Emerit J, Chaudiere J. Free radicals and lipid peroxidation in cell pathology. In: Miquel J, Quintanilha AT, Weber H, editors. Handbook of free radicals and antioxidants in biomedicine. 6th ed. Boca Raton: CRC Press; 1984. p. 177–85.

34. Polla BS, Jacquier-Sarlin MR, Kantengwa S, Mariethoz E, Hennet T, Russo-Marie F, et al. TNFα alters mitochondrial membrane potential in L929 but not in TNFα-resistant L929.12 cells: relationship with the expression of stress proteins, annexin 1 and superoxide dismutase activity. Free Rad Res 1996;25: 125–31.

35. Penning LC, Lagerberg JW, Van Dierendonck JH, Cornelisse CJ, Dubbelman TM. The role of DNA damage and inhibition of poly(ADP-ribosyl)ation in loss of clonogenicity of murine L929 fibroblasts, caused by photodynamically induced oxidative stress. Cancer Res 1994;54:5561–7.

36. Bereznowski Z. Effect of methyl methacrylate on mitochondrial function and structure. Int J Biochem 1994;26:1119–27.

37. Vallittu PK, Ruyter IE, Buykuilmaz S. Effect of polymerization temperature and time on the residual monomer content of denture base polymers. Eur J Oral Sci 1998;106:588–93.

38. Vallittu PK, Miettinen V, Alakuijala P. Residual monomer content and its release into water from denture base materials. Dent Mater 1995;11:338–42.

39. Bowen RL. Compatibility of various materials with oral tissues. I: The components in composite restorations. J Dent Res 1979; 58:1493–503.